Journal of
Synchrotron Radiation

ISSN 1600-5775

Received 11 September 2013
Accepted 29 December 2013

Object image correction using an X-ray dynamical diffraction Fraunhofer hologram

Minas K. Balyan

Faculty of Physics, Department of Solid State Physics, Yerevan State University, Alex Manoogian 1, Yerevan 0025, Armenia. E-mail: mbalyan@ysu.am

Taking into account background correction and using Fourier analysis, a numerical method of an object image correction using an X-ray dynamical diffraction Fraunhofer hologram is presented. An example of the image correction of a cylindrical beryllium wire is considered. A background correction of second-order iteration leads to an almost precise reconstruction of the real part of the amplitude transmission coefficient and improves the imaginary part compared with that without a background correction. Using Fourier analysis of the reconstructed transmission coefficient, non-physical oscillations can be avoided. This method can be applied for the determination of the complex amplitude transmission coefficient of amplitude as well as phase objects, and can be used in X-ray microscopy.

Keywords: X-ray Fraunhofer holography; X-ray dynamical diffraction; image reconstruction; X-ray microscopy.

1. Introduction

In the work of Balyan (2013) an X-ray dynamical diffraction Fraunhofer holographic scheme was proposed and theoretically investigated. It was shown that an object image can be reconstructed by illumination of an X-ray dynamical diffraction Fraunhofer hologram with visible light. In the mentioned work the corresponding references are given as well.

Numerical methods of reconstruction are important for phase objects (Snigirev *et al.*, 1995; Momose, 1995). Balyan (2014) presented a numerical method of reconstruction of an object image using a dynamical diffraction Fraunhofer hologram. Analytical as well as iteration methods of reconstruction of the real direct image were presented. However, the background correction of the reconstructed image in relation to the virtual image and autocorrelation was ignored.

In this work we take into account the background correction. An example of background correction of the image will be presented. The Fourier method for avoiding non-physical oscillations of the numerically reconstructed object image will be discussed.

2. Background correction of the numerically reconstructed object image

In the X-ray dynamical diffraction Fraunhofer hologram recording scheme (Balyan, 2013) an object is placed in the path of an incident plane monochromatic X-ray wave. In a thick perfect crystal (of thickness T), under the condition of two-wave dynamical Laue-case symmetrical diffraction, the reference plane wave and the object wave interfere and an interference pattern is formed on the exit surface of the crystal. Only the weakly absorbing mode of σ-polarization can be taken into account. The intensity distribution of the diffracted wave is (Balyan, 2013)

$$I_h = \left|E_h\right|^2 = \left|E_{h\,\mathrm{ref}}\right|^2 + E_{h\,\mathrm{ref}}\,E^*_{h\,\mathrm{obj}} + E^*_{h\,\mathrm{ref}}\,E_{h\,\mathrm{obj}} + \left|E_{h\,\mathrm{obj}}\right|^2, \quad (1)$$

where $E_{h\,\mathrm{ref}}$ is the amplitude of the reference wave and $E_{h\,\mathrm{obj}}$ is the amplitude of the object wave. The third term of the right-hand side after reconstruction gives the real direct image of the object and the second term gives the virtual image of the object.

The analyses given by Balyan (2013, 2014) show that by multiplying (1) by $\exp[i\pi(p-x)^2/(2D)]$ (the coordinate axis Ox is antiparallel to the diffraction vector and Oz is perpendicular to the entrance surface of the crystal) and integrating by x over the hologram plane one obtains an integral equation for the amplitude complex transmission coefficient $t(x, y)$ of the object {y is the coordinate perpendicular to the diffraction plane and x is the coordinate of the observation point of the object and differs from the integration variable x in $\exp[i\pi(p-x)^2/(2D)]$}. Here p is a parameter and $D = \Lambda T \tan^2\theta$, where Λ is the extinction length and θ is the Bragg angle. The parameter p and the coordinate x of the observation point of the object are connected by the relation $p + k\cos\theta\Delta\theta D/\pi = x$, where $\Delta\theta$ is the deviation from the Bragg exact angle. We assume that the experimental values of I_h are known. After integration one can write $E_{\mathrm{rec}} = \sum_{j=1}^{4} E_{\mathrm{rec}\,j}$. Here the term on the left-hand side corresponds to the integration of I_h, and the terms on the right-hand side correspond to the integration of each of the terms on the right-hand side of (1). For expressions for E_{rec} and $E_{\mathrm{rec}\,j}$, see Balyan (2014).

For the zero-order approximation, ignoring $E_{\mathrm{rec2,4}}$, one can find (Balyan, 2014)

$$t^{(0)}(x, y) = 1 - \left[E_{\mathrm{rec}}(p, y) - E_{\mathrm{rec1}}\right]/E_{\mathrm{rec3abs}}(p, y). \quad (2)$$

Here E_{rec3abs} is E_{rec3} for a completely absorbing object [for such an object $t(x, y) = 0$] of the same size as the considered object.

For the first-order approximation of the amplitude transmission coefficient, taking into account the background correction and the result obtained by Balyan (2014), one can write

$$t_{\rm cr}^{(1)}(x,y) = t^{(1)}(x,y) + \left[E_{\rm rec2}^{(0)}(p,y) + E_{\rm rec4}^{(0)}(p,y)\right]/E_{\rm rec3abs}(p,y), \quad (3)$$

where, instead of the unknown $S(x,y) = 1 - t(x,y)$ in the expressions of the background terms $E_{\rm rec2}^{(0)}(p,y)$ and $E_{\rm rec4}^{(0)}(p,y)$ obtained by the zero-order approximation, $S^{(0)}(x,y) = 1 - t^{(0)}(x,y)$ is used, and $t^{(1)}(x,y)$ is the first-order approximation without background correction. The subscript 'cr' means corrected.

For the second-order iteration, taking into account the background correction, we have

$$t_{\rm cr}^{(2)}(x,y) = t^{(2)}(x,y) + \left[E_{\rm rec2}^{(1)}(p,y) + E_{\rm rec4}^{(1)}(p,y)\right]/E_{\rm rec3abs}(p,y), \quad (4)$$

where, instead of the unknown $S(x,y)$ in the expressions of the background terms $E_{\rm rec2}^{(1)}(p,y)$ and $E_{\rm rec4}^{(1)}(p,y)$ obtained by the first-order approximation, $S^{(1)}(x,y)$ is used, and $t^{(2)}(x,y)$ is the second-order approximation without background correction.

3. Fourier analysis of the reconstructed transmission coefficient

The iteration procedure leads to non-physical oscillations of the reconstructed transmission coefficient. These oscillations affect the higher-order harmonics of the Fourier transform of the transmission coefficient. If one cuts the higher-order harmonics affected by the oscillations and takes the inverse Fourier transform, a smoothed transmission coefficient can be obtained. Thus we first calculate the Fourier transforms

$$F\left[\mathrm{Re}\, t_{\rm cr}^{(2)}(x,y)\right] = \int_{x_{1\rm re}}^{x_{2\rm re}} \exp(iqx)\ \mathrm{Re}\, t_{\rm cr}^{(2)}(x,y)\, \mathrm{d}x, \quad (5)$$

$$F\left[\mathrm{Im}\, t_{\rm cr}^{(2)}(x,y)\right] = \int_{x_{1\rm im}}^{x_{2\rm im}} \exp(iqx)\ \mathrm{Im}\, t_{\rm cr}^{(2)}(x,y)\, \mathrm{d}x. \quad (6)$$

Here $x_{1\rm re}$ and $x_{2\rm re}$ are the coordinates of the points between which the oscillations of the real part of the transmission coefficient are included, and $x_{1\rm im}$ and $x_{2\rm im}$ have the same sense for the imaginary part. By cutting the functions $F\left[\mathrm{Re}\, t_{\rm cr}^{(2)}(x,y)\right]$ and $F\left[\mathrm{Im}\, t_{\rm cr}^{(2)}(x,y)\right]$ at the appropriate places and taking the inverse Fourier transform, a smoothed transmission coefficient is obtained.

4. Example

For the case of a Si(220) reflection, $\lambda = 0.71$ Å (17.46 keV) radiation, $\Delta\theta = 0$, $T = 5$ mm, σ-polarization is taken, and $\mu T = 7.3$. As an object we take a circular cylindrical beryllium wire with its axis perpendicular to the diffraction plane. The radius of the wire $R_{\rm obj} = 30$ µm. The refractive index $n = 1 - \delta + i\beta$. For beryllium, $\delta = 1.118 \times 10^{-6}$ and $\beta = 2.69 \times 10^{-10}$. The amplitude transmission coefficient is

$$t(x,y) = \exp\left\{-2ik(\delta - i\beta)\left[R_{\rm obj}^2 - x^2\cos^2\theta\right]^{1/2}\right\}. \quad (7)$$

Now we must numerically reconstruct (7) using the method described above. Using (7) we can calculate the intensity distribution on the Fraunhofer hologram of the considered object [see Fig. 2 of Balyan (2014)]. Using formulae (2)–(4), the second-order iteration of the amplitude transmission coefficient is calculated, taking into account the background corrections. In Figs. 1(*a*) and 1(*b*) the real and imaginary parts of the obtained amplitude transmission coefficient are compared with the exact values; by partially avoiding the non-physical oscillations of the second-order iteration, the average values $\bar{t}_{\rm cr}^{(2)}(x) = [t_{\rm cr}^{(2)}(x) + t_{\rm cr}^{(1)}(x)]/2$ are shown. Let us compare Fig. 1(*a*) of this paper with Fig. 6(*a*) of Balyan (2014) (the reconstructed real part

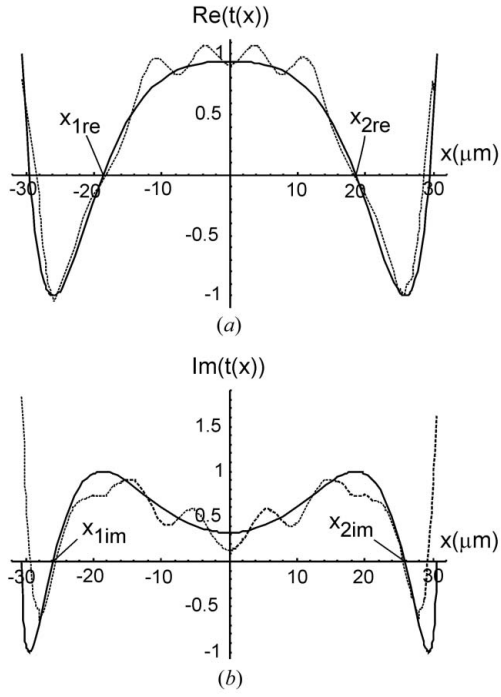

Figure 1
Comparison of the reconstructed second-order iteration with the exact amplitude complex transmission coefficient of the beryllium wire taking into account background correction. (*a*) Real parts, (*b*) imaginary parts. The solid lines show the exact values and the dashed lines show the second-order iteration.

without background correction). After correction, the minima in the ranges -30 µm $\le x \le -20$ µm and 20 µm $\le x \le 30$ µm almost exactly coincide with the minima of the exact values. Moreover, near the edges ($x = -30$ µm and $x = 30$ µm), the corrected values almost equal 1 (the exact value) whereas the non-corrected values are less than 0.5. The background corrections lead to an almost precise reconstruction of the real part. Now let us compare Fig. 1(*b*) with Fig. 6(*b*) of the paper by Balyan (2014) (imaginary part without correction). After correction, the minima in the ranges -30 µm $\le x \le -20$ µm and 20 µm $\le x \le 30$ µm decrease and are closer to the minima of the exact values. At the edges ($x = -30$ µm and $x = 30$ µm), the corrected values also decrease and are closer to the exact values. The correction improves the imaginary part. Non-physical oscillations can be removed using Fourier analysis. According to Figs. 1(*a*) and 1(*b*), we take $x_{1\rm re} = -18.7$ µm, $x_{2\rm re} = 18.7$ µm and $x_{1\rm im} = -25.7$ µm, $x_{2\rm im} = 25.7$ µm. In Figs. 2(*a*) and 2(*b*) the real parts of the functions $F\left[\mathrm{Re}\, \bar{t}_{\rm cr}^{(2)}(x,y)\right]$ and $F\left[\mathrm{Im}\, \bar{t}_{\rm cr}^{(2)}(x,y)\right]$ are shown (the imaginary parts are small and can be ignored). Now, by taking these functions in the interval $-0.5\ \mu\mathrm{m}^{-1} \le q \le 0.5\ \mu\mathrm{m}^{-1}$ (*i.e.* cutting them outside the mentioned interval) and performing an inverse Fourier transform, one finds the smoothed real part of the transmission coefficient in the interval -18.7 µm $\le x \le 18.7$ µm and the smoothed imaginary part of this function in the interval -25.7 µm $\le x \le 25.7$ µm [outside these intervals we take the values $\bar{t}_{\rm cr}^{(2)}(x)$]. The results are shown in Figs. 3(*a*) and 3(*b*).

5. Conclusion

A numerical method of an object image reconstruction using an X-ray dynamical diffraction Fraunhofer hologram and taking into account background correction is presented. To avoid non-physical oscillations the Fourier transform method is used. As an example, the reconstruction of an image of a cylindrical beryllium wire is consid-

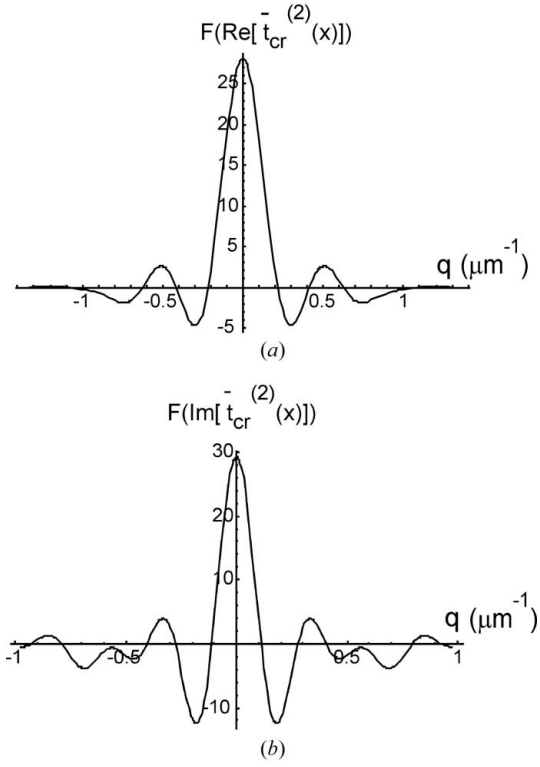

Figure 2
Fourier transforms of the real (*a*) and imaginary (*b*) parts of $\bar{t}_{cr}^{(2)}(x)$.

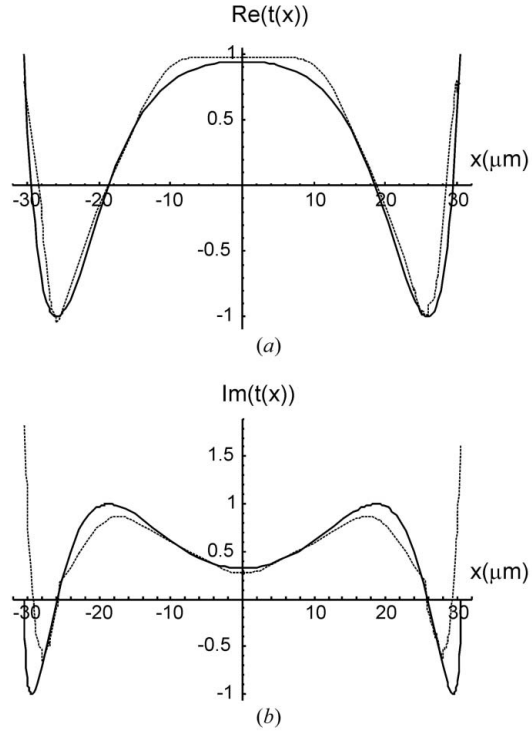

Figure 3
Smoothed real (*a*) and imaginary (*b*) parts of $\bar{t}_{cr}^{(2)}(x)$ are compared with the exact values of $t(x)$. Solid lines show the exact values and dashed lines show the smoothed reconstructed values.

ered. Calculations including background corrections almost precisely reconstruct the real part of the amplitude transmission coefficient and improve the imaginary part.

This method can be applied for the determination of the complex amplitude transmission coefficients of amplitude as well as phase objects, and can be used in X-ray microscopy.

References

Balyan, M. (2013). *J. Synchrotron Rad.* **20**, 749–755.
Balyan, M. K. (2014). *J. Synchrotron Rad.* **21**, 127–130.
Momose, A. (1995). *Nucl. Instrum. Methods Phys. Res. A*, **352**, 622–628.
Snigirev, A., Snigireva, I., Kohn, V., Kuznetsov, S. & Schelokov, I. (1995). *Rev. Sci. Instrum.* **68**, 5486–5492.